INTERNATIONAL JOURNAL OF PRECISION ENGINEERING AND MANUFACTURING Vol. 18, No. 5, pp. 705-710 MAY 2017 / 705

REGULAR PAPER

DOI: 10.1007/s12541-017-0084-6
ISSN 2234-7593 (Print) / 2005-4602 (Online)

Fracture Behavior of Adhesive Interface at TDCB Aluminum Foam Specimen with the Type of Mode III

Jung Ho Lee[1] and Jae Ung Cho[2,#]

1 Department of Mechanical Engineering, Graduate School, Kongju National University, 1223-24, Cheonan-daero, Seobuk-gu, Cheonan-si, Chungcheongnam-do, 31080, South Korea
2 Division of Mechanical & Automotive Engineering, Kongju National University, 1223-24, Cheonan-daero, Seobuk-gu, Cheonan-si, Chungcheongnam-do, 31080, South Korea
Corresponding Author / E-mail: jucho@kongju.ac.kr, TEL: +82-41-555-9123

KEYWORDS: Adhesive interface, Aluminum foam, Fracture, Specimen Thickness, TDCB , Type of mode III

In this study, the fracture property is investigated with the configuration of tapered double cantilever beam different from that of the existing double cantilever beam. Aluminum TDCB (Tapered Double Cantilever Beam) specimens of mode III-type are bonded by an adhesive. The specimens had thicknesses as a variable which were 35 mm, 45 mm, and 55 mm, respectively. In the case of the specimen with a thickness of 35 mm, the maximum reaction force was shown to be about 0.4 kN when the forced displacement had progressed by about 8 mm, while the maximum reaction force of about 0.45 kN occurred in case of the specimen with a thickness of 45 mm when the forced displacement proceeded by about 7 mm, and the maximum reaction force of about 0.54kN occurred in case of the specimen with a thickness of 55mm when the forced displacement proceeded by about 7 mm. In addition, the static fracture analysis was performed for its verification by using the finite element analysis of ANSYS program, where it was affirmed that the experimental results and the simulation analysis results were shown to be similar. Based on this observation, it is considered that the simulation analysis data could be applied to the bonded interfaces of actual porous materials.

Manuscript received: November 16, 2016 / Revised: December 27, 2016 / Accepted: December 29, 2016

1. Introduction

With the development of industries at many kinds of fields today, materials constituting various machines and mechanical apparatuses as well as mechanical structures are diversified withtheir characteristics. Unlike the past when machines were produced simply by using steels only, not only improvement of machine performance but also weight reduction is currently devoted by using special alloy steels, composite materials and light-weight materials. Furthermore, weight reduction problems of materials are being emerged anew as the weight reduction of transportation means such as automobiles and the correspondingfuel economy problems are intensified. As a the fastening method for machines and mechanical structures in such a weight reduction, a fastening method by using only adhesives rather than the existing method using bolts and nuts attracts public attention. Aluminum foam is a very suitable super-light metal material for the relevant fastening method, and is the materialwhich can be used in diversified fields such as light-weight structural material for buildings, shock-absorbing material applicable to vehicle bumpers or some frames for shock absorption, engine noise preventive fixture and other sound absorption andsoundproofing materials and the special filter for heat exchangers. In this study, the characteristics of aluminum foam bonded structures were studied by using closed-type aluminum foam which is employed mainly as a shock-absorbing material.[1-7] However, in case of structures fastened by such adhesives only, fracture toughness data for the joined joint part is essentially required for their safe use. Particularly, since fracture characteristics of the bonded interfaces of aluminum foam as a porousmaterial can be different as compared with nonporous materials, studies on the fracture toughness of aluminum foam bonded interfaces may be considered very important.[8-12] As this specimen has the configuration of tapered double cantilever beam, one side is fixed and the other side is free. This kind of cantilever beam supports the load through the bending moment and shearing force happening at fixed support and is used as the fixed structure of the bridge and tower and the wings of airplane. Accordingly, in this study, Tapered Double Cantilever Beam (TDCB) specimens of mode III-type with single-lap bonding method were designed using closed-type aluminum foam produced by Foam Tech Co., Ltd. on the basis of British standard (BS 7991) and ISO international specification (ISO 11343). As such, for designed specimens having different Thicknesses, the static fracture

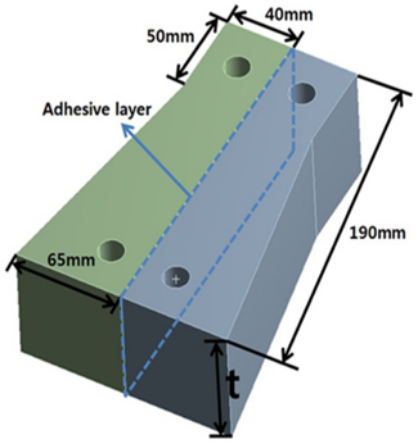

Fig. 1 Configuration of TDCB specimen

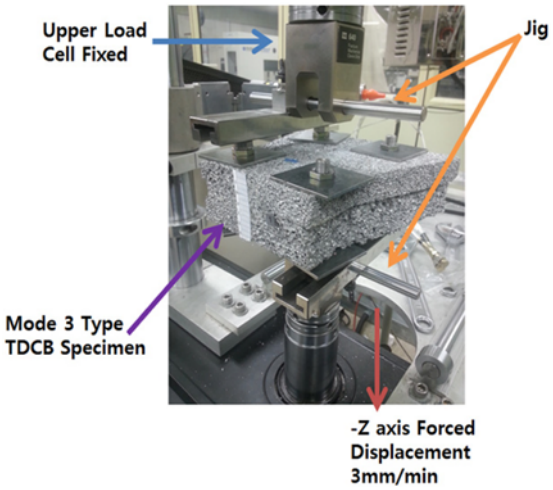

Fig. 2 Experimental setup for static experiment

tests were performed by using a tensile tester. As the crack is propagated along the bonded interface at the TDCB composite under the impact fatigue load, the fracture behavior is analyzed in this study. Also, the static fracture analysis was conducted for its verification by using the finite element analysis program of ANSYS and the shear strengths of bonded interfacing for the bonded TDCB structures made of aluminum foam as a porous material could be evaluated on the basis of the derived results.[13-19]

The study of static fracture due to the configuration of tapered cantilever beam is carried out and this fracture property is derived and investigated.

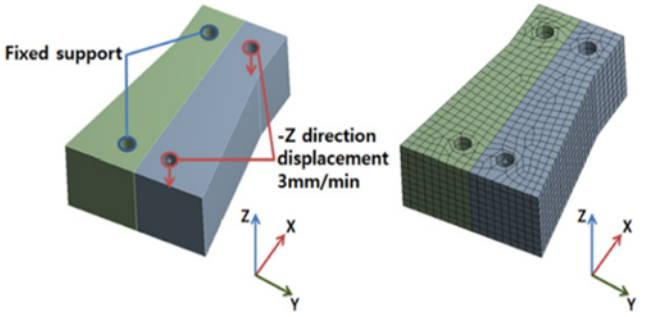

Fig. 3 Boundary condition (left) and mesh of model (right)

2. Research Method

2.1 Research model

To match the intent of this study, a TDCB-type specimen model of single-lap bonding method was designed on the basis of the drawings specified in British standard 7991 : 2001. As shown in the following Fig. 1, the TDCB specimen model was designed with the Thickness value t as a variable, where the lateral length of the upper side in the model was 80 mm, the lateral length of the lower side as 130 mm, the longitudinal length as 190 mm. In case of 50 mm, the value was determined on the basis of shape factor, and 3 types of models were designed at an interval of 10 mm for the Thickness values of 35 mm, 45 mm, and 55 mm, respectively.

2.2 Experiment conditions

Fig. 2 below shows the static experiment method for TDCB specimens with the type of mode III to verify the simulation analysis results. Tensile tester employed in this study was manufactured by MTS Company. Since it was not possible to directly connect the specimens to the upper load cell and the lower load cell due to the experimental method of this study, a jig was additionally manufactured to interconnect the specimen and the tensile tester as seen in the figure. The upper load cell was fixed while a forced displacement of 3 mm/min in z-axis direction was applied to the lower load cell to perform the experiment.

Table 1 Numbers of nodes and elements of analysis models

Thickness of specimen model	Nodes	Elements
35 mm	10327	1859
45 mm	11982	2268
55 mm	14673	3083

Table 2 Material properties

Property	Value
Density (kg/m^3)	400
Young's modulus (MPa)	2,374
Poisson's ratio	0.29
Yield strength (MPa)	1.8
Shear strength (MPa)	0.92

2.3 Boundary condition for the simulation analysis

Fig. 3 schematically shown below, represents the boundary conditions and meshes, respectively applied to the TDCB specimen model. With the assumption that each specimen is connected and fixed to the tensile tester, the holes on one side of the specimen model were fixed by applying a fixed support condition. With the assumption that forced displacement for the holes on the other side proceeded by the lower load cell, the analysis was performed by pulling one side of the test piece in Z axis direction with the forced displacement of 3 mm/min. The numbers of nodes and elements for each specimen model is

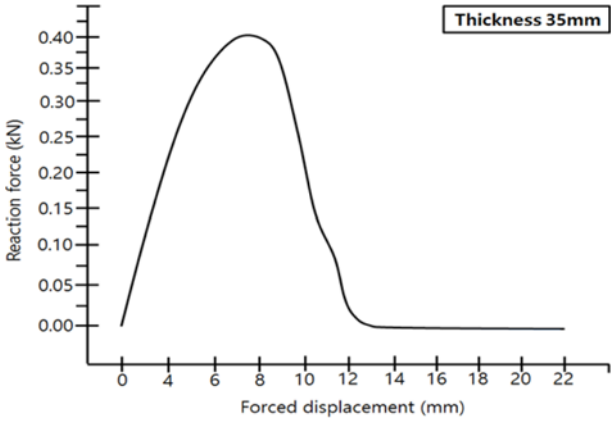

Fig. 4 Graph of reaction force due to forced displacement of the static experiment (Thickness of specimen is 35 mm)

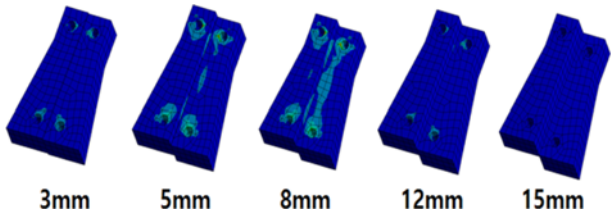

Fig. 5 Change of the equivalent stress according to the progress of forced displacement (Thickness of specimen is 35 mm)

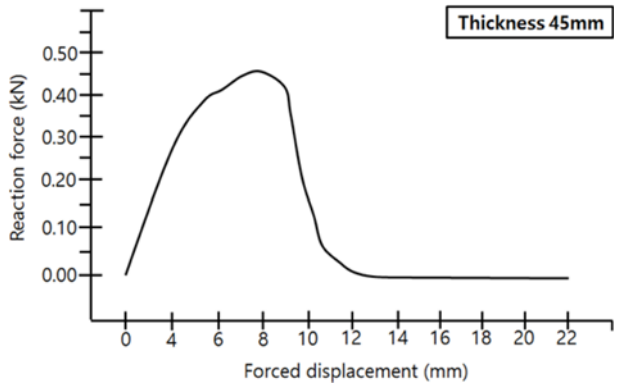

Fig. 6 Graph of reaction force due to forced displacement of the static experiment (Thickness of specimen is 45 mm)

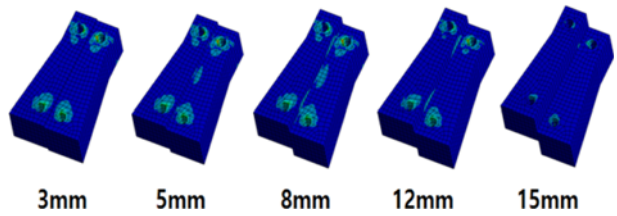

Fig. 7 Change of the equivalent stress according to the progress of forced displacement (Thickness of specimen is 45 mm)

denoted in the following Table 1. For the model employed in this study, Al-SAF40 was used as aluminum foam, and material property values for the specimen model applied in the simulation analysis are shown in the following Table 2. Also, the adhesive coated onto adhesive layers of the specimen was an aerosol-type adhesive with an adhesion strength of 0.4 MPa.

3. Research Results

3.1 Experimental results for the test piece with a Thickness of t = 35 mm

Fig. 4 diagrammatically shown below shows the static experiment results for the specimen with a Thickness of t = 35 mm, where reaction forces due to forced displacement are diagrammatically shown as a graph. When the forced displacement proceeded by about 7 mm, the maximum reaction force could be affirmed to occur in the specimen, at which the maximum reaction force was shown to be about 0.4 kN. After the occurrence of maximum reaction force, the adhesive force at the bonded interface of test piece was gradually reduced, and the reaction force was shown to become the value of 0 after the bonded interface of the test piece was completely separated when the forced displacement proceeded by about 12 mm. Also, Fig. 5 shows the analysis results of the specimen with a Thickness of t = 35 mm, showing the stress contour occurring in the specimen as a result of the progress with forced displacement. While forced displacement proceeded, it can be affirmed that the stresses occurred in the specimen were gradually reduced to disappear.

3.2 Experimental results for the test piece with a Thickness of t = 45 mm

Fig. 6 diagrammatically shows the static experiment results as a graph for the specimen with a Thickness of t = 45 mm, displaying reaction force values due to forced displacement. According to the results of performing the experiments, it can be affirmed that a similar tendency to that for the specimen with a Thickness of t = 35 mm was observed, where the maximum reaction force was shown to occur in the specimen when the forced displacement was proceeded by about 8 mm, with the maximum reaction force at this time being about 0.45 kN. From the time where the maximum reaction force occurred, the adhesive force at the bonded interface of the specimen was drastically reduced, and the reaction force can be affirmed to have become the value of 0 as the bonded interface of the test piece was completely separated when the forced displacement was proceeded by about 13 mm. The following Fig. 7 shows the analysis results for the test piece with a Thickness of t = 45 mm, displaying a stress contour occurred in the specimen as the result of progress with forced displacement. Stresses can be affirmedto be gradually reduced with the progress of forced displacement.

3.3 Experimental results for the test piece with a Thickness of t = 55 mm

Fig. 8 shows the static experiment results for the specimen with a Thickness of t = 55 mm, where reaction forces are graphed as a function of forced displacement. According to the experimental results,

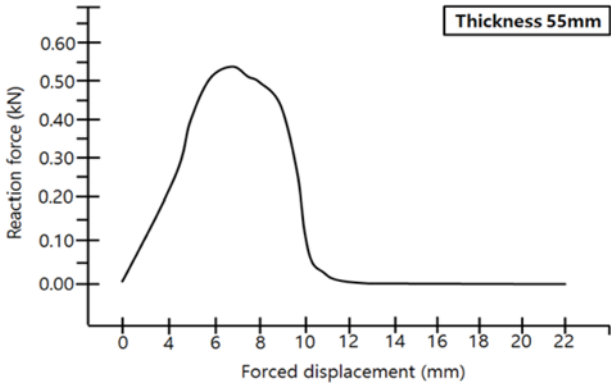

Fig. 8 Graph of reaction force due to forced displacement of the static experiment (Thickness of specimen is 55 mm)

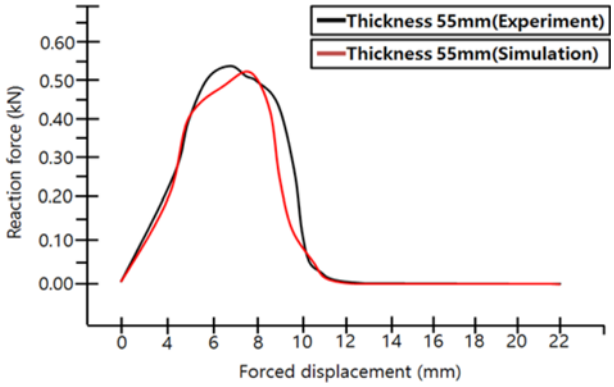

Fig. 10 Comparison between experimental and simulation analysis data (Thickness of specimen is 55 mm)

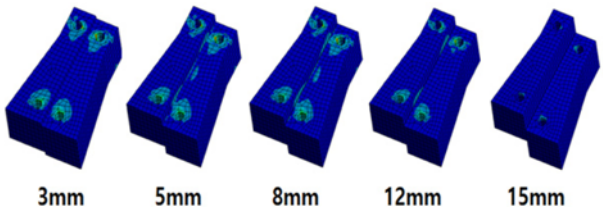

Fig. 9 Change of the equivalent stress according to the progress of forced displacement (Thickness of specimen is 55 mm)

it can be affirmed to show a similar tendency as those for the specimens with Thicknesses of t = 35 mm and t = 45 mm, and the maximum reaction force can be affirmed to occur in the specimen at about 0.54 kN when the forced displacement proceeded by about 7 mm. After the occurrence of maximum reaction force, the adhesive force at the bonded interface of the specimen was gradually reduced as with other specimens, and the reaction force can be affirmed to become the value of 0 as the bonded interface of the specimen was completely separated when the forced displacement proceeded by about 13 mm. The following Fig. 9 shows the analysis results for the test piece with a Thickness of t = 55 mm, displaying a stress distribution occurring in the specimen with the progress in forced displacement. With the progress of forced displacement, the gradual disappearance of the stress occurring in the specimen can be affirmed.

3.4 Comparison between experiment and analysis for the test piece with a Thickness of t = 55 mm

In this study, the static analysis using simulation was performed to verify the experimental results of static fracture. As the study result, the data at the Thicknesses of 35 mm, 45 mm and 55 mm have the similar trends all together. As an example of the simulation static analysis results for this purpose, a graph for the corresponding reaction force data in the static fracture experiment for the specimen of a Thickness t = 55 mm when the forced displacement of 3 mm/min was applied and a graph for reaction force data in static analysis are shown in Fig. 10 According to the analysis results, it can be affirmed that the maximum reaction force was shown in a similar way to the simulation analysis when the forced displacement was proceeded by about 8 mm. The maximum reaction force at this time is about 0.52 kN, and shown to have no large difference when compared with the experimental result of about 0.54 kN. From the time of occurrence of the maximum reaction force, the adhesive force at the bonded interface in the specimen can be affirmed to be gradually reduced as in the static fracture experiments, and the reaction force was observed to become the value of 0 as the bonded interface was completely separated after the forced displacement proceeded by about 12 mm. Also, the point where the bonded interface was completely separated became about 13 mm in case of static fracture experiment, and about 12 mm in the case of static analysis, affirming that there was no large difference. According to the comparison results, the gradual increase in reaction forces due to forced displacement until the maximum reaction force occurs and can be affirmed in both the static fracture experiment and the static analysis. The maximum reaction force can be affirmed to occur when the forced displacement proceeds by about 7 mm and 8 mm, respectively. Considering the graph, however, it can be seen that a difference exists between the analysis and the experimental data after the occurrence of maximum reaction force, which is attributed to the adhesive inertia impeding progress of forced displacement as the adhesive coated onto the bonded interfaces of the specimen remained without disappearing when the experiments were performed.

Also, as shown by the corresponding figures, the curves of reaction forces are bent like stair. It is thought that the bonding inertia of adhesive sprayed on the bonded interface of specimen prevents the specimen from proceeding with the enforced displacement. Likewise, as is explained above at Figs. 4, 6 and 8, it is estimated that the curves of reaction forces are bent like stair at these graphs due to the same reason.

Fig. 11 shows stresses at the bonded interface for the static analysis when the maximum reaction force occurred in the specimen with a Thickness of t = 55 mm, stress contour due to forced displacement and appearance of experiment implementation for the comparison of analysis. The above figure shows the stresses at the bonded interface of the specimen when the maximum reaction force occurred, while the two figures below represent the stress contour occurred in the specimen with the progress of forced displacement and the process of experiment implementation. When the maximum reaction force occurred in the specimen, the stress at the bonded interface was shown to be about

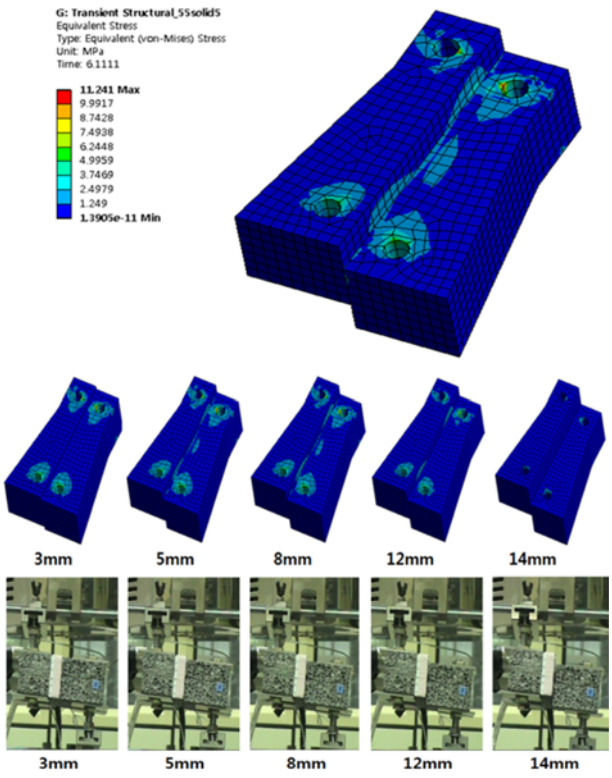

Fig. 11 Stress at bonded interface in a simulation analysis when the maximum reaction force occurred in the specimen with a Thickness of t = 55 mm, stress contour due to forced displacement and experimental implementation process for the comparison of analysis

1.249 MPa, and the contour of stresses due to the progress of forced displacement as well as the shearing process of bonded interface in the test piece can be affirmed in the figures below.

4. Conclusion

As the experimental and simulation results of fracture behavior on the structures of TDCB Jointed with aluminum foam in tearing mode, the following conclusions are made in this study:

1. In static fracture experiments, occurrence of the maximum reaction force was observed when a constant forced displacement of about 7 to 8 mm was proceeded in all TDCB specimens with different Thicknesses of t = 35 mm, 45 mm and 55 mm. In the case of the static fracture analysis performed for its verification, the maximum reaction force was also observed to occur similarly when the forced displacement was proceeded by about 8 mm.

2. The maximum reaction force for each TDCB specimen was shown to be about 0.4 kN in the case of the specimen with a Thickness of t = 35 mm, about 0.45 kN for the specimen with a Thickness of t = 45 mm, about 0.54 kN for the specimen with a Thickness of t = 55 mm, and hence the maximum reaction force of a specimen was affirmed to be increased as Thicknesses of specimens were increased.

3. According to the study results, the static fracture experiment result and the static fracture analysis result for specimens were confirmed to be similar. Therefore, it is considered that data for other variables can be simply secured on the basis of the accumulated data without the separate experimental processes, and that mechanical characteristics can be analyzed for the bonded interfaces in the joined TDCB structures with mode III type. It is thought that this study result on the adhesive interface of foam structure can be devoted to systemize the fracture property. Hereafter, this study aims at securing and supplying the basic data for safer use and design at the composite parts of automobile, ship and airplane where the bonding method using the adhesive is applied.

ACKNOWLEDGEMENT

This research was supported by Basic Science Research Program through the National Research Foundation of Korea (NRF) funded by the Ministry of Education, Science and Technology (2015R1D1A1A01 057607).

REFERENCES

1. Lefanti, R., Ando, M., and Sukumaran, J., “Fatigue and Damage Analysis of Elastomeric Silent Block in Light Aircrafts,” Materials & Design, Vol. 52, pp. 384-392, 2013.

2. Hu, H., Lu, W.-J., and Lu, Z., “Impact Crash Analyses of an Off-Road Utility Vehicle - Part II: Simulation of Frontal Pole, Pole Side, Rear Barrier and Rollover Impact Crashes,” International Journal of Crashworthiness, Vol. 17, No. 2, pp. 163-172, 2012.

3. Han, M.-S., Choi, H.-K., Cho, J.-U., and Cho, C.-D., “Experimental Study on the Fatigue Crack Propagation Behavior of DCB Specimen with Aluminum Foam,” Int. J. Precis. Eng. Manuf., Vol. 14, No. 8, pp. 1395-1399, 2013.

4. Zhang, Y.-j. and Yang, C.-s., “FEM Analyses for Influences of Stress-Chemical Solution on THM Coupling in Dual-Porosity Rock Mass,” Journal of Central South University, Vol. 19, No. 4, pp. 1138-1147, 2012.

5. Cho, J. U., Hong, S. J., Lee, S. K., and Cho, C., “Impact Fracture Behavior at the Material of Aluminum Foam,” Materials Science and Engineering: A, Vol. 539, pp. 250-258, 2012.

6. Pirondi, A. and Nicoletto, G., “Fatigue Crack Growth in Bonded DCB Specimens,” Engineering Fracture Mechanics, Vol. 71, No. 4, pp. 859-871, 2004.

7. Shokrieh, M. M., Heidari-Rarani, M., and Rahimi, S., “Influence of Curved Delamination Front on Toughness of Multidirectional DCB Specimens,” Composite Structures, Vol. 94, No. 4, pp. 1359-1365, 2012.

8. Blackman, B. R. K., Dear, J. P., Kinloch, A. J., MacGillivray, H., Wang, Y., et al., “The Failure of Fibre Composites and Adhesively Bonded Fibre Composites Under High Rates of Test,” Journal of Materials Science, Vol. 31, No. 17, pp. 4467-4477, 1996.

9. Cho, J.-U., Kinloch, A., Blackman, B., Rodriguez, S., Cho, C.-D., and Lee, S.-K., "Fracture Behaviour of Adhesively-Bonded Composite Materials Under Impact Loading," Int. J. Precis. Eng. Manuf., Vol. 11, No. 1, pp. 89-95, 2010.

10. Cooper, V., Ivankovic, A., Karac, A., McAuliffe, D., and Murphy, N., "Effects of Bond Gap Thickness on the Fracture of Nano-Toughened Epoxy Adhesive Joints," Polymer, Vol. 53, No. 24, pp. 5540-5553, 2012.

11. Ghaffarzadeh, H. and Nikkar, A., "Explicit Solution to the Large Deformation of a Cantilever Beam Under Point Load at the Free Tip Using the Variational Iteration Method-II," Journal of Mechanical Science and Technology, Vol. 27, No. 11, pp. 3433-3438, 2013.

12. Goncalves, J. P. M., De Moura, M., and De Castro, P., "A Three-Dimensional Finite Element Model for Stress Analysis of Adhesive Joints," International Journal of Adhesion and Adhesives, Vol. 22, No. 5, pp. 357-365, 2002.

13. Jiang Z., Wan S. and Song A., "An Alternative Solution for the Edge Moment Factors of the Unbalanced Adhesive Single-Lap Joint in Tension," International Journal of Adhesion and Adhesives, Vol. 75, pp. 1-16, 2017.

14. Crocombe, A. D. and Richardson, G., "Assessing Stress State and Mean Load Effects on the Fatigue Response of Adhesively Bonded Joints," International Journal of Adhesion and Adhesives, Vol. 19, No. 1, pp. 19-27, 1999.

15. Ohno, N., Okumura, D., and Niikawa, T., "Long-Wave Buckling of Elastic Square Honeycombs Subject to In-Plane Biaxial Compression," International Journal of Mechanical Sciences, Vol. 46, No. 11, pp. 1697-1713, 2004.

16. British Standard Institution, "Determination of the Mode I Adhesive Fracture Energy GIC of Structure Adhesives Using the Double Cantilever Beam (DCB) and Tapered Double Cantilever Beam (TDCB) Specimens," BS 7991, 2001.

17. Kim, S.-S., Han, M.-S., Cho, J.-U., and Cho, C.-D., "Study on the Fatigue Experiment of TDCB Aluminum Foam Specimen Bonded with Adhesive," Int. J. Precis. Eng. Manuf., Vol. 14, No. 10, pp. 1791-1795, 2013.

18. Michailidis, N., Stergioudi, F., Omar, H., and Tsipas, D., "An Image-Based Reconstruction of the 3D Geometry of an Al Open-Cell Foam and Fem Modeling of the Material Response," Mechanics of Materials, Vol. 42, No. 2, pp. 142-147, 2010.

19. Pradeep, K. R., Rao, B. N., Srinivasan, S. N., and Balasubramaniam, K., "Interface Fracture Assessment on Honeycomb Sandwich Composite DCB Specimens," Engineering Fracture Mechanics, Vol. 93, pp. 108-118, 2012.